















## SPECIAL ISSUE ARTICLE

# Combining adhesive and nonadhesive injectable hydrogels for intervertebral disc repair in an ovine discectomy model

Christopher J. Panebianco<sup>1,2</sup>  | Caroline Constant<sup>3</sup>  | Andrea J. Vernengo<sup>3,4</sup>  | Dirk Nehrass<sup>3</sup>  | Dominic Gehweiler<sup>3</sup>  | Tyler J. DiStefano<sup>1</sup>  | Jesse Martin<sup>5</sup> | David J. Alpert<sup>5</sup>  | Saad B. Chaudhary<sup>1</sup>  | Andrew C. Hecht<sup>1</sup>  | Alan C. Seifert<sup>6</sup>  | Steven B. Nicoll<sup>5</sup>  | Sibylle Grad<sup>3</sup>  | Stephan Zeiter<sup>3</sup>  | James C. Iatridis<sup>1</sup> 

<sup>1</sup>Leni and Peter W. May Department of Orthopaedics, Icahn School of Medicine at Mount Sinai, New York, New York, USA

<sup>2</sup>Department of Orthopaedic Surgery, University of Pennsylvania, Philadelphia, Pennsylvania, USA

<sup>3</sup>AO Research Institute Davos, Davos, Switzerland

<sup>4</sup>Department of Chemical Engineering, Rowan University, Glassboro, NJ, USA

<sup>5</sup>Department of Biomedical Engineering, The City College of New York, New York, New York, USA

<sup>6</sup>Biomedical Engineering and Imaging Institute, Icahn School of Medicine at Mount Sinai, New York, New York, USA

## Correspondence

James C. Iatridis, Department of Orthopaedics, Icahn School of Medicine at Mount Sinai, One Gustave L. Levy Place, Box 1188, New York, NY 10029, USA.

Email: [james.iatridis@mssm.edu](mailto:james.iatridis@mssm.edu)

## Funding information

AO Foundation; AOSpine; National Institute of Arthritis and Musculoskeletal and Skin Diseases, Grant/Award Numbers: F31 AR077385, R01 AR057397, R01 AR080096

## Abstract

**Background:** Intervertebral disc (IVD) disorders (e.g., herniation) directly contribute to back pain, which is a leading cause of global disability. Next-generation treatments for IVD herniation need advanced preclinical testing to evaluate their ability to repair large defects, prevent reherniation, and limit progressive degeneration. This study tested whether experimental, injectable, and nonbioactive biomaterials could slow IVD degeneration in an ovine discectomy model.

**Methods:** Ten skeletally mature sheep (4–5.5 years) experienced partial discectomy injury with cruciate-style annulus fibrosus (AF) defects and 0.1 g nucleus pulposus (NP) removal in the L1–L2, L2–L3, and L3–L4 lumbar IVDs. L4–L5 IVDs were intact controls. IVD injury levels received: (1) no treatment (Injury), (2) poly (ethylene glycol) diacrylate (PEGDA), (3) genipin-crosslinked fibrin (FibGen), (4) carboxymethylcellulose–methylcellulose (C-MC), or (5) C-MC and FibGen (FibGen + C-MC). Animals healed for 12 weeks, then IVDs were assessed using computed tomography (CT), magnetic resonance (MR) imaging, and histopathology.

**Results:** All repaired IVDs retained ~90% of their preoperative disc height and showed minor degenerative changes by Pfirrmann grading. All repairs had similar disc height loss and Pfirrmann grade as Injury IVDs. Adhesive AF sealants (i.e., PEGDA and FibGen) did not herniate, although repair caused local endplate (EP) changes and inflammation. NP repair biomaterials (i.e., C-MC) and combination repair (i.e., FibGen + C-MC) exhibited lower levels of degeneration, less EP damage, and less severe inflammation; however, C-MC showed signs of herniation via biomaterial expulsion.

**Conclusions:** All repair IVDs were noninferior to Injury IVDs by IVD height loss and Pfirrmann grade. C-MC and FibGen + C-MC IVDs had the best outcomes, and may be appropriate for enhancement with bioactive factors (e.g., cells, growth factors, and

Christopher J. Panebianco and Caroline Constant contributed equally to this study.

This is an open access article under the terms of the [Creative Commons Attribution-NonCommercial](https://creativecommons.org/licenses/by-nc/4.0/) License, which permits use, distribution and reproduction in any medium, provided the original work is properly cited and is not used for commercial purposes.

© 2023 The Authors. *JOR Spine* published by Wiley Periodicals LLC on behalf of Orthopaedic Research Society.

miRNAs). Such bioactive factors appear to be necessary to prevent injury-induced IVD degeneration. Application of AF sealants alone (i.e., PEGDA and FibGen) resulted in EP damage and inflammation, particularly for PEGDA IVDs, suggesting further material refinements are needed.

#### KEYWORDS

annulus fibrosus repair, carboxymethylcellulose–methylcellulose, fibrin, hydrogels, injectable biomaterials, intervertebral disc, nucleus pulposus repair, ovine discectomy model, poly(ethylene glycol) diacrylate

## 1 | INTRODUCTION

Spine pathologies are among the most frequently encountered problems in clinical practice, which can cause disabilities and considerable economic losses.<sup>1</sup> Furthermore, lower back and neck pain are among the most common reasons for seeking primary medical advice.<sup>2</sup> Among individuals experiencing back pain, intervertebral disc (IVD) disorders are the most predominant painful conditions diagnosed.<sup>3,4</sup> Despite extensive research to improve the treatment and prevention of spinal disorders, the prevalence of low back pain remains high, with an incidence reaching more than 30% of the adult population.<sup>5–7</sup> These high incidences of low back pain have resulted in rising annual costs for spine clinical care in the last decades.<sup>1,8,9</sup>

Back pain is a multifaceted condition, but IVD degeneration is generally accepted as one of the main causes of low back pain.<sup>4</sup> During IVD degeneration, the IVD is subjected to many modifications, with disc herniation being the most common functional alteration, and a possible source of direct pain.<sup>4</sup> When IVDs herniate, there is a gross migration of the central nucleus pulposus (NP) tissue through defects in the outer annulus fibrosus (AF) tissue. The standard of care for symptomatic herniation with associated radicular pain is discectomy; whereby, a surgeon will remove the herniated NP tissue.<sup>10–12</sup> Clinical trials have demonstrated that the outcomes of discectomy patients are superior to nonoperative controls<sup>10,11</sup>; however, some patients experience complications like reherniation and recurrent pain are common.<sup>13,14</sup> New surgical procedures have been reported to improve surgical outcomes by limiting the amount of tissue removed during discectomy and reducing soft tissue trauma, which can reduce postoperative complications.<sup>15</sup> Nevertheless, optimizing the amount of tissue removed during surgical procedures has limits, and this solution will not repair herniation-induced defects. AF closure devices, such as the Barricaid® (Intrinsic Therapeutics, Woburn, MA), have been developed to prevent reherniation complications, yet this device has been reported to cause subsidence, damaged the endplates (EPs) of adjacent vertebral bodies, and did not heal injured IVDs.<sup>16–18</sup> Instead, novel therapeutic interventions are needed to repair injured IVDs.

Injectable biomaterials are a promising therapeutic option to repair or replace degenerated IVD tissue because they are minimally invasive, gel in situ, and fill irregularly shaped defects.<sup>19,20</sup> Various injectable biomaterials have been proposed to mimic the structural

and biomechanical properties of IVD tissue.<sup>21</sup> To replace the nucleus pulposus (NP), which is the gelatinous, proteoglycan-rich core of the IVD, hydrogels composed of polyvinyl alcohol,<sup>22</sup> poly(L-lactic acid),<sup>23</sup> poly(N-isopropylacrylamide),<sup>24–26</sup> alginate,<sup>27</sup> hyaluronic acid,<sup>28</sup> collagen,<sup>29</sup> and carboxymethylcellulose<sup>30,31</sup> have been studied. These hydrogel NP replacements can help restore tissue hydration, disc height, and promote biomechanical restoration<sup>24,32</sup>; however, most NP replacement hydrogels are nonadhesive or weakly adhesive and prone to herniation through AF defects.<sup>33,34</sup> To address this, adhesive AF sealants have become another important research area for IVD repair. In these approaches, hydrogels composed of collagen,<sup>35,36</sup> albumin,<sup>37</sup> cyanoacrylate,<sup>38</sup> poly(ethylene glycol) diacrylate (PEGDA),<sup>39</sup> and fibrin<sup>40–42</sup> are used to fill AF defects and crosslink in situ to form covalent bonds with the surrounding tissue. These results in a mechanically competent barrier designed to prevent herniation of native NP tissue or intradiscally implanted hydrogels.

Recent studies have explored using combinations of NP hydrogels and adhesive AF sealants to repair injured IVDs.<sup>37,43,44</sup> For example, Sloan et al. used hyaluronic acid hydrogels as an NP replacement hydrogel in combination with photocrosslinked collagen as an adhesive AF sealant to repair a sheep model of discectomy. Their results demonstrated that the combination repair resulted in superior IVD hydration, biomechanical properties, and preserved lamellar AF morphology compared to the individual treatments alone.<sup>44</sup> Another study by Hom et al. used a combination of carboxymethylcellulose–methylcellulose (C-MC) as an NP replacement and genipin-crosslinked fibrin (FibGen) as an adhesive AF sealant to repair injured bovine IVDs in situ. Their results showed that IVDs repaired with FibGen and C-MC exhibited failure at supraphysiological stress levels, suggesting low herniation risk.<sup>43</sup> These studies highlight the importance of conducting further preclinical investigations on how NP hydrogels and adhesive AF sealants can be used to repair critically sized AF defects.

The aim of this study was to evaluate the in vivo performance of four injectable IVD repair biomaterial strategies that were previously developed by our group: (1) PEGDA, (2) FibGen, (3) C-MC, and (4) a combination of FibGen and C-MC (FibGen + C-MC). PEGDA<sup>39</sup> and FibGen<sup>41</sup> hydrogels were chosen as AF sealants because they are tunable, cytocompatible, integrate well into injured IVDs through covalent bonding, and have low herniation risk. FibGen was also shown to restore some biomechanical properties in a short-term organ culture model of IVD injury and repair.<sup>40</sup> C-MC was chosen as a nonadhesive

NP replacement because it is tunable, cytocompatible, mimics mechanical properties of the NP, and restores disc height under fatigue bending in bovine motion segments.<sup>32</sup> FibGen + C-MC was also tested because FibGen could potentially prevent the herniation risk of nonadhesive C-MC<sup>32</sup> and this biomaterial combination was validated *ex vivo* using a large animal model of IVD injury.<sup>43</sup> Our hypothesis was that treating injured IVDs with FibGen + C-MC would prevent disc height loss, radiographic signs of degeneration, and histopathological signs of degeneration resulting from a partial discectomy injury in an *in vivo* ovine discectomy model.

## 2 | MATERIALS AND METHODS

### 2.1 | Study design and preclinical model overview

This study included 10 skeletally mature female Swiss White Alpine sheep ( $N = 10$  sheep) randomly assigned to one of two subsequent treatment groups ( $N = 5$  sheep per group). Using a lateral retroperitoneal surgical approach, a cruciate AF defect with 0.1 g NP removal was created at the L1–L2, L2–L3, and L3–L4 lumbar IVD levels. This AF defect model was used to simulate a partial discectomy, which is the standard of care for symptomatic IVD herniation.<sup>10</sup> IVD injury levels in the first group were systematically assigned to one of the following treatments: (1) no treatment (Injury), (2) poly (ethylene glycol) diacrylate (PEGDA), or (3) genipin-crosslinked fibrin (FibGen). In the second investigation, AF defect levels were systematically assigned to the following groups: (1) Injury, (2) repair with carboxymethylcellulose–methylcellulose (C-MC), or (3) repair with C-MC and FibGen (FibGen + C-MC). The L4–L5 IVD level served as an Intact control for both investigations (Figure 1).

During the 12-week observation period, animal welfare was monitored by clinical examination, and the lumbar spine was monitored by clinical computed tomography (CT). Postmortem analyses included magnetic resonance (MR) imaging and histopathology. Outcomes of interest were degenerative changes observed by medical imaging (i.e., disc height loss, Pfirrmann grading, and MR image evaluation) and

degenerative changes observed by histopathologic examination. At the end of the study period, sheep were euthanized by an overdose of pentobarbital (7.5 g, intravenously).

### 2.2 | Animals

Ten skeletally mature female Swiss Alpine sheep (age range: 4–5.5 years, mean weight:  $83 \pm 6$  kg) were used in this study. Sheep were kept under a 12 h dark/light cycle, fed hay, and given mineral supplements. Two weeks before starting the study, sheep were acclimated to the local conditions and animal caretakers. Preoperatively, sheep received a complete physical assessment by a veterinarian, including a complete blood cell count and CT examination of the lumbar spine. Only sheep in good physical health and free of degenerative disc disease were included in the study. Postoperatively, sheep were housed in groups of 3–5 under the same light and feeding conditions listed above. Postoperative clinical physical examinations using an animal welfare assessment score sheet were performed twice daily for 3 days. Daily evaluations were performed for the following 4 days. Weekly assessments and weighing were performed throughout the remainder of the experiment.

The study adhered to the ARRIVE reporting standard for research (Data S1: ARRIVE Guidelines). This study was compliant with the Directive 2010/63/EU, approved by Cantonal authorities in Graubünden, Switzerland (Permission #: 19/2020 and 19/2021), and performed in an Association for Assessment and Accreditation of Laboratory Animal Care (AAALAC) accredited facility.

### 2.3 | Hydrogel fabrication

This study tested two adhesive AF sealants (i.e., PEGDA and FibGen) and one nonadhesive NP repair biomaterial (i.e., C-MC).

PEGDA IVDs were repaired with a two-part strategy, which used dual-modified hyaluronic acid to adhere PEGDA hydrogels to IVD tissue, as previously described.<sup>39</sup> Briefly, hyaluronic acid was oxidized

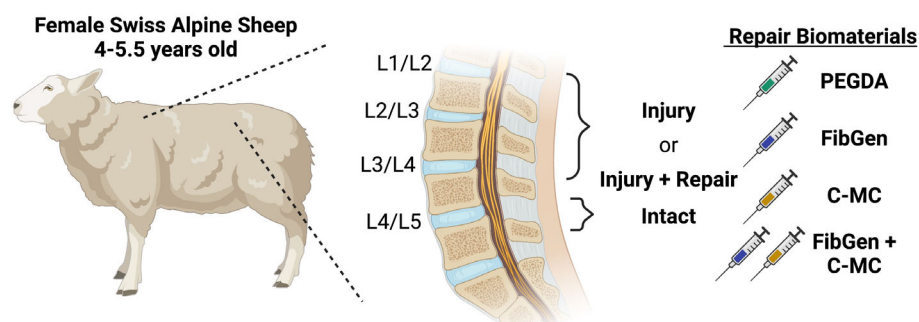


**FIGURE 1** Schematic representation of sheep injury and repair model. Intervertebral discs (IVDs) were injured using a cruciate defect with 0.1 g of nucleus pulposus (NP) removal. L1/L2, L2/L3, and L3/L4 IVDs were injured and systematically assigned to one of the following groups: (1) Injury, (2) repair with poly(ethylene glycol) diacrylate (PEGDA), (3) repair with genipin-crosslinked fibrin (FibGen), (4) repair with carboxymethylcellulose–methylcellulose (C-MC), and (5) combination repair with C-MC as an NP replacement and FibGen as an annulus fibrosus (AF) sealant (FibGen + C-MC). The L4/L5 IVD was kept as an intact control for all animals.

using sodium periodate (Sigma Aldrich, St. Louis, MO) and methacrylated using methacrylic anhydride (Sigma Aldrich) to form HAMA. Interpenetrating network PEGDA hydrogels were prepared using a 1:1 double-barrel syringe with a mixing tip (Pacific Dental, Walnut, CA). One barrel contained 20 kDa PEGDA (15% v/v, Sigma Aldrich), thrombin (10 U/mL, Sigma Aldrich), and N,N,N',N'-tetramethylethylenediamine (TEMED, 40 mM, Bio-Rad Laboratories, Hercules, CA). The second barrel contained fibrin (5 mg/mL, Sigma Aldrich), ammonium persulfate (APS, 40 mM, Acros Organics, Fair Lawn, NJ), fibronectin (10 µg/mL, Sigma Aldrich), and Oxyrase-EC (3.3% v/v, Oxyrase, Mansfield, OH). All components were dissolved in 1X phosphate-buffered saline (PBS, Thermo Fisher Scientific Company, Bohemia, NY).

FibGen hydrogels were prepared using a 4:1 double-barrel syringe with a mixing tip (Pacific Dental), as previously described.<sup>45,46</sup> The large barrel contained bovine fibrinogen (140 mg/mL, Sigma Aldrich), while the small barrel contained thrombin (28 U/mL, Sigma Aldrich) and genipin (6 mg/mL, Wako Chemicals, Richmond, VA). All components were dissolved in 1X PBS.

C and MC hydrogels were prepared as previously described.<sup>31,47</sup> Briefly, C (Sigma Aldrich) and MC (Sigma Aldrich) were methacrylated using methacrylic anhydride. After methacrylation, CMC-MC hydrogels were prepared using a 1:1 double barrel syringe with a mixing tip (Sulzer Mixpac AG, Salem, NH). Each barrel contained C-MC (3% w/v), while one barrel contained APS (20 mM) and the other contained TEMED (20 mM). All components were dissolved in 1X PBS.

All powders were sterilized by ultraviolet light for 1 h under rotation and all liquid components were filter sterilized. To ensure that results from PEGDA and FibGen repair were not caused by infection, we tested our components for sterility and found that none of the tested biomaterials produced microbial growth over a 14-day culture. Additionally, regular veterinary examinations throughout the study showed that there were no clinical signs of infection.

## 2.4 | Surgical intervention

Sheep underwent IVD injury surgery, including the creation of an AF cruciate defect and 0.1 g NP removal, using a left lateral retroperitoneal surgical approach under general anesthesia, as previously described.<sup>48</sup> Prior to general anesthesia induction, sheep were maintained off-feed for 36–48 h. Sheep were sedated with Detomidine (0.04 mg/kg, Equisedan, E. Graeb AG, Switzerland), then general anesthesia was induced using an intravenous mixture of midazolam (0.2 mg/kg; Midazolam Sintetica<sup>®</sup>, Sintetica S.A., Mendrisio, Switzerland) and ketamine (4 mg/kg; Ketazol-100; Roche Pharma AG, Basel, Switzerland). Endotracheal intubation was performed, and general anesthesia was maintained using Sevoflurane volatile liquid anesthetic. Preoperative analgesia was provided by Carprofen (4 mg/kg; Carprodolor, Virbac AG, Switzerland), and lumbosacral epidural analgesia with Buprenorphine (0.005 mg/kg, Bupaq, Streuli Pharma AG, Uznach, Switzerland) and lidocaine (Lidocain 2% Streuli, Streuli Pharma AG).

The left lateral IVD was surgically exposed and a cruciate AF defect was created with two cuts at 45° from the longitudinal IVD axis in the left ventrolateral AF of the L1–L2, L2–L3, and L3–L4 IVDs using a scalpel blade a No. 11. This resulted in a full thickness annulotomy, which spanned 8-mm wide and 8-mm deep. After creating the AF defect, the NP was fenestrated and Beck rongeurs (2-mm wide, 5-mm length) were used to remove 0.1 g of NP tissue. Removed NP was weighted with a high precision scale ( $\pm 0.001$  g) and kept for histopathological analysis. The L4–L5 IVD was left intact for all animals to be used as an Intact control. The operating surgeons were blinded to the study groups during IVD injury creation.

AF defect levels were systematically assigned to one of the biomaterial repair groups: (1) Injury, (2) PEGDA, (3) FibGen, (4) C-MC, or (5) FibGen + C-MC. Biomaterials were prepared as described above (Section 2.3), and approximately 200 µL of each biomaterial/biomaterial combination was injected into each injured IVD. The precise volume was not measured due to small variations in IVD size. For PEGDA IVDs, approximately 150 µL of the HAMA aldehyde solution (10% w/v) was slowly injected into the AF defect using a 5 mL syringe with a 20G  $\times$  1–1/2" BD PrecisionGlide™ Needle (Beckton, Dickinson and Company, Franklin Lakes, NJ). After allowing the Schiff base formation to occur on the IVD tissue surface for 5 min, the HAMA aldehyde was aspirated from the IVD space. Then, the PEGDA prepolymer solution was injected into the AF defect.<sup>39</sup> For FibGen IVDs, FibGen syringes were prepared, as described above (Section 2.3), and injected into the IVD defect. For C-MC IVDs, C-MC syringes were prepared, as described above (Section 2.3), and injected into the NP space of the IVD defect. For FibGen + C-MC IVDs, C-MC and FibGen were injected into the IVD defect in two parts, as previously described.<sup>43</sup> Briefly, the C-MC hydrogel was injected first into the NP space, and then the remaining AF defect was filled using FibGen.

Following IVD injury and repair, surgical incisions were closed in multiple continuous layers using USP 0 (muscle layers) and USP 2-0 and 3-0 (subcutaneous and skin) resorbable sutures. After surgery, analgesia was provided by repeated injections of Carprofen (4 mg/kg), Buprenorphine (0.005 mg/kg), and transdermal Fentanyl [2 µg/kg/h; Fentanyl-Mepha<sup>®</sup> (Fentanyl Patches), Mepha Pharma AG]. Antibiotic prophylaxis regimen included peri-operative sodium-ceftiofur (2.2 mg/kg; EXCENEL 1 g<sup>®</sup>/Zoetis Schweiz GmbH, Switzerland), then long-acting ceftiofur (6.6 mg/kg; Naxcel<sup>®</sup> 200 mg/mL Rind/Zoetis Schweiz GmbH, Switzerland) administered at the end of surgery.

## 2.5 | In vivo clinical CT

In vivo clinical CT scans of the lumbar spine were acquired using a Revolution EVO CT system (GE Medical Systems, Switzerland) to evaluate disc height changes over time. Scans were acquired preoperatively, immediately postoperatively (W0), 4 weeks postinjury (W4), W8, and after euthanasia at W12. Sheep were sedated and anesthetized before in vivo clinical CT imaging as described above (Section 2.4). The CT images were obtained with a slice thickness and spacing of 0.625 and 0.312 mm, respectively. Tube voltage was

120 kVp and the tube current was 300 mA. Disc height was measured by a blinded observer using Amira software (Amira 6.5, FEI SAS, Thermo Fisher Scientific) as previously described.<sup>48</sup> Briefly, lumbar vertebrae were semi-automatically segmented, and then the shortest distance between each point on the cranial IVD extremity and the caudal IVD extremity was measured for each IVD. The average disc height was calculated as the arithmetic mean of all points along an individual IVD, which was approximately 5000 points. Postoperative disc heights were expressed as a percentage of the preoperative disc heights. Therefore, a relative disc height of less than 100% postoperatively would represent a disc height loss when compared to preoperative values.

## 2.6 | Ex vivo MR imaging

Following euthanasia, lumbar spines were harvested for ex vivo MR imaging. MR images were acquired using a 1.5 MRI scanner (Phillips Medical Systems, Best, The Netherlands) with a sense-body imaging coil. The sequencing protocol consisted of unenhanced T1-weighted, T2-weighted, and short tau inversion recovery (STIR) sequences in the axial, coronal, and sagittal planes. MR images were reviewed by two orthopedic surgeons, who used the Pfirrmann grading system to identify clinically meaningful changes in IVD degeneration.<sup>49</sup> Each surgeon provided a Pfirrmann grade for each disc in a blinded fashion. In the case where the surgeons provided different grades, the mean Pfirrmann grade was used for further analysis.

MR images were also scored by an experienced IVD researcher and an MR physicist with spine imaging experience for a detailed assessment of NP, AF, and endplate (EP) quality. Both individuals were blinded and conferred to ensure agreement of interpretations before providing one combined score for each category. The categories, listed in Table 1, were adapted from Constant et al.,<sup>48</sup> and qualitative assessments were assigned numerical scores to allow for statistical analysis. For each category, IVDs were scored from 0 to 2 or 0 to 3, depending on the category. For the “Herniation” category, herniations were further characterized by NP herniation or biomaterial expulsion. These MR findings were further validated using histopathology.

## 2.7 | Histopathological analysis

Harvested lumbar segments were fixed in 70% ethanol, dehydrated, embedded in methylmethacrylate, and sectioned to approximately 300 µm. Sections were then stained for Safranin-O/Fast Green, using standard protocols. Stained sections were graded by one certified veterinary pathologist, blinded to the study groups, using a grading system adapted from Shu et al. to evaluate IVD degeneration (Table 2).<sup>50</sup> The grading consisted of six categories: proteoglycan depletion, IVD structure and lesion morphology, cellular morphology, blood vessel ingrowth, cellular influx into the lesion, and cleft formation. For each category, IVDs were assigned a grade from 0 to 4. In addition to the

**TABLE 1** Radiographic scoring of normal and pathological ovine intervertebral discs (IVDs).

Grade	Histopathologic features
<b>(A) NP Intensity</b>	
0	NP appears bright
1	NP appears dimmer
2	NP appears faint
3	NP appears dark
<b>(B) NP Shape</b>	
0	NP shape is round and healthy
1	NP shape is elongated
2	NP shape is disrupted
<b>(C) IVD Condition</b>	
0	AF has no heterogeneity
1	AF has minor/focal heterogeneity
2	AF has moderate heterogeneity
3	AF has severe/extensive heterogeneity
<b>(D) Herniation</b>	
0	No herniation present
1	Herniation or fissure is present
2	Herniation and fissure are both present
<b>(E) EP Changes</b>	
0	EP changes are absent
1	Minor EP changes
2	Moderate EP changes
3	Extensive EP changes
<b>(F) Marrow changes</b>	
0	Marrow or Modic changes are absent
1	Marrow or Modic changes are present
<b>(G) Inflammation</b>	
0	Inflammation is absent
1	Minor inflammation is present
2	Moderate inflammation is present
3	Extensive inflammation is present
<b>(H) Ectopic calcification</b>	
0	Ectopic calcification is absent
1	Mild ectopic calcification is present
2	Extensive ectopic calcification is present

Abbreviations: AF, annulus fibrosus; EP, cartilaginous endplate; NP, nucleus pulposus.

semi-quantitative grading, qualitative assessments of collagen fibril organization were conducted using polarized light microscopy. A total histopathological score was calculated by summing grades across all categories, excluding the cellular morphology score. This category was removed from the analysis because it was found to be the only parameter similar to all IVDs, including Intact control. Therefore, this category was interpreted as an incidental background finding in adult sheep lumbar IVD, not a pathological change. Additionally, findings at

**TABLE 2** Histopathological scoring of normal and pathological ovine intervertebral discs (IVDs).

Grade	Histopathologic features
<i>(A) Safranin O/fast green proteoglycan staining</i>	
0	Fast green staining only of oAF, intermediate Safranin O staining of iAF, intense Safranin O staining in NP, and well-defined CEP staining. Alternate AF lamellae discernable due to differing Fast Green staining intensities of adjacent lamellae
1	Slightly reduced Safranin O staining of mAF/iAF in vicinity of lesion, Fast Green staining of oAF only, normal Safranin O staining of NP and CEP
2	Moderately reduced Safranin O staining of mAF/iAF in vicinity of lesion, fast green staining of oAF only, normal Safranin O staining of NP and CEP
3	Reduced patchy Safranin O staining around lesion, fast green staining in oAF (no Safranin O staining)
4	Reduced Safranin O staining in NP compared to Intact IVD, very faint, or no Safranin O staining in oAF/mAF, fast green staining only in oAF
<i>(B) IVD Structure/lesion characteristics</i>	
0	Normal IVD structure with well-defined annular lamellae, central NP, and CEP
1	Lesion evident in mAF, normal NP morphology
2	Lesion evident in mAF/iAF, lesion but may not be apparent in oAF due to spontaneous repair, iAF lamellae may be inverted and have anomalous distortions in normal lamellar architecture
3	Bifurcation/propagation of lesion from mAF/iAF into NP margins, mild delamination, when more extensive may lead to concentric tears between lamellae in mAF/iAF
4	Propagation of lesion into NP, with disruption in normal NP structure, distortion of annular lamellae into atypical arrangements-severe delamination, separation of translamellar cross bridges
<i>(C) Cellular morphology</i>	
0	Normal, sparse distribution of typical single AF and NP fibrochondrocytes
1	Small groups of rounded chondrocytic cells (2–4 cells/group) in iAF, occasional cell division in resident iAF, and NP cells
2	Moderate increase in well-defined groups of rounded chondrocytic cells (4–8/group) with penetrating blood vessels associated with the lesion site, well-defined chondroid cell colonies in NP contained within a dense basophilic matrix with little fibrillar material evident around the cells contrasting with NP cells
3	Marked increase in less defined groups of rounded chondrocytic cells (>8/group) with penetrating blood vessels associated with the lesion site, well-defined chondroid cell colonies in NP (<50 cells/colony) contained within a dense basophilic matrix with little fibrillar material evident around the cells contrasting with NP cells
4	Numerous cell clones, chondroid cell nests in NP containing >50 cells
<i>(D) Blood vessel ingrowth</i>	
0	Very occasional vessels in outermost annular lamellae, occasional capillaries in CEP
1	Low number of blood vessels in oAF and mAF
2	Moderate number of blood vessels in oAF and mAF
3	Large number of blood vessels in iAF
4	Extensive ingrowth of vessels in iAF/mAF and along lesion margins
<i>(E) Influx of inflammatory cells into the lesion site</i>	
0	Normal cell distribution in oAF, mAF, iAF, and NP
1	Slight influx of cells mainly in oAF
2	Moderate influx of cells throughout AF
3	Large influx of cells throughout AF
4	Extensive influx of cells throughout AF particularly in iAF and around lesion
<i>(F) Formation of clefts in vicinity to lesion (mainly radially oriented)</i>	
0	No clefts in AF
1	Small cleft area in AF
2	Moderate cleft area in AF
3	Large cleft area in AF
4	Vast cleft area in AF and also in NP

Abbreviations: AF, annulus fibrosus; CEP, cartilaginous endplate; iAF, inner AF; mAF, mid-AF; oAF, outer AF; NP, nucleus pulposus.



the vertebral bone were recorded according to four categories: EP Safranin-O reduction, EP discontinuation or thinning, vertebral body osteolysis, and vertebral body callus formation or periosteal reaction. For each category, IVDs were assigned a grade from 0 to 4. IVDs were also assessed for herniation of NP tissue and repair biomaterials to validate findings observed and quantified via MR imaging.

A semi-quantitative scoring scheme was developed to assess damage to adjacent vertebral bodies. Safranin O reduction, EP thinning, osteolysis, and callus formation were all scored by a certified histopathologist in a blinded fashion. For each category listed, samples were assigned a score of 0 (no change), 1 (mild change), 2 (moderate change), 3 (marked change), and 4 (severe change).

NP samples collected during surgery were also analyzed for mineralization using von Kossa staining. Pronounced von Kossa staining was interpreted as bone tissue deriving from surgical iatrogenic vertebral EP trauma.

## 2.8 | Statistical analysis

Power analysis was conducted with R (Indianapolis, IN) using the “pwr2” package to approximate the sample sizes necessary to detect large effect sizes. GraphPad Prism software Version 9 (GraphPad Software, San Diego, CA) was used to conduct all statistical analyses, with results reported as mean  $\pm$  standard deviation. The nonparametric Kruskal–Wallis one-way analysis of variance (ANOVA) with Dunn's multiple comparison test was used to determine significant differences in Pfirrmann, MR, and histopathology grading. For Pfirrmann grading, interobserver agreement percentage was calculated using Cohen's kappa coefficient. The nonparametric Kruskal–Wallis two-way ANOVA with Dunn's multiple comparison test was used to determine significant differences in disc height over time. Post-hoc analyses compared Injury and repair (i.e., PEGDA, FibGen, C-MC, and FibGen + C-MC) IVDs to Intact IVDs, and compared repair IVDs to Injury IVDs. For all statistics,  $\alpha = 0.05$  was used for significance. Throughout the manuscript, the word “difference” is used to mean statistically different ( $p < 0.05$ ), with appropriate symbol notation on accompanying graphs. Specific  $p$  values were only included in the text to highlight statistical trends ( $0.05 < p < 0.10$ ).

## 3 | RESULTS

### 3.1 | Animals experience successful surgical interventions

The surgical intervention was successful in all sheep and resulted in a surgically induced left-sided IVD defect. Defects were either kept empty (Injury;  $n = 10$  IVDs) or treated with PEGDA ( $n = 5$  IVDs), FibGen ( $n = 5$  IVDs), C-MC ( $n = 5$  IVDs), or a combination of C-MC and FibGen (FibGen + C-MC;  $n = 5$  IVDs). Injury and repair conditions were compared to Intact controls ( $n = 10$  IVDs). Based on the histopathological analysis of the removed NP tissue, minimal (63.3% of

IVDs;  $n = 19/30$  IVDs) to moderate (36.7% of IVDs;  $n = 11/30$  IVDs) EP trauma was induced during the procedure but was not detectable on postoperative CT examination. General anesthesia recovery was uneventful in all cases. Based on clinical physical examination and welfare scoring results, no clinical signs of back pain were observed during the entire study duration, and all sheep gained weight postoperatively.

### 3.2 | Injury and repair IVDs experience comparably low disc height loss

Successful IVD repair biomaterials should prevent injury-induced disc height loss; thus, in vivo clinical CT was used to evaluate disc height changes up to 12 weeks post-injury (W12). All disc height measurements were normalized to their respective preoperative values. Interestingly, all IVDs experienced a slight disc height increase after partial discectomy injury, which was attributed to a combination of soft tissue disruption, swelling, and anesthesia effects. As expected, partial discectomy caused Injury IVDs to show significantly lower disc heights than Intact controls at W4, W8, and W12 (Figure 2). All IVD repair biomaterials performed similarly at W0; however, the relative disc height of PEGDA, FibGen, and C-MC IVDs was significantly less than Intact controls by W4. By W8, FibGen + C-MC IVDs also had significantly reduced disc heights than Intact IVDs. Although biomaterial repair could not prevent injury-induced disc height loss, repaired IVDs did not experience disc height loss greater than Injury IVDs. Furthermore, all IVDs maintained a relative disc height of at least 90% of their original disc height with no significant changes between W4 to W12.

### 3.3 | PEGDA and FibGen hydrogels cause degenerative MR changes

T1- and T2-weighted MR imaging was used to assess degenerative IVD changes at W12 in postmortem sheep (Figure 3A). MR images were first assessed using the Pfirrmann grading system, which is a useful tool for identifying clinically meaningful, macroscale degenerative IVD changes.<sup>49</sup> The interobserver agreement percentage for the Pfirrmann grading, calculated using Cohen's kappa coefficient, was 88.9%. This is indicative of excellent agreement and validates the precision of our grading measurements.<sup>51</sup> As anticipated, Injury IVDs had significantly higher Pfirrmann grades than Intact IVDs, indicating that partial discectomy injury resulted in IVD degeneration (Figure 3B). All repaired IVDs had similar Pfirrmann grades to Injury IVDs, which were significantly greater than Intact IVDs. These findings demonstrate that the tested IVD repair biomaterials could not reverse macroscale degenerative changes caused by partial discectomy injury, although degenerative changes were mild and did not result in clinically meaningful differences between the groups. Follow-up comprehensive MR image analyses were conducted to determine if there were local changes that might be meaningful.

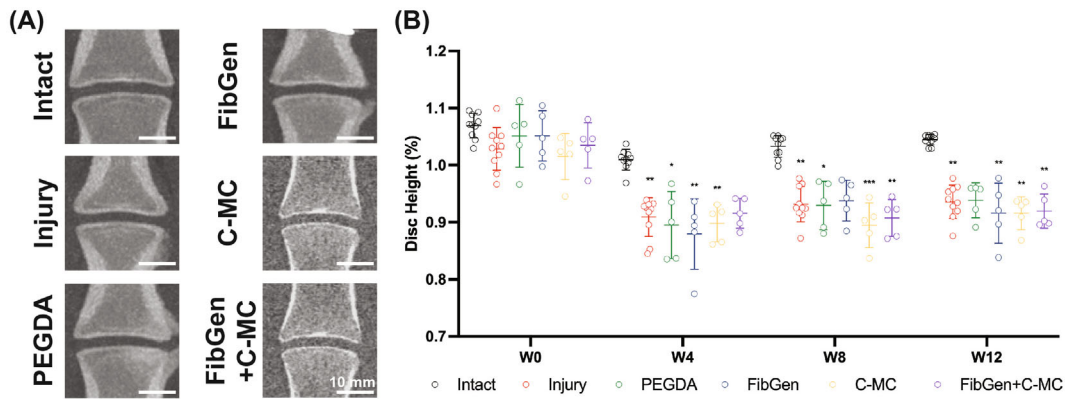


**FIGURE 2** Repaired IVDs maintained at least 90% of their preoperative disc height by W12. (A) Representative computed tomography (CT) images at 12 weeks post-injury (W12). Scale bar = 10 mm. (B) Disc height normalized to preoperative values. \**p* < 0.05, \*\**p* < 0.01, and \*\*\**p* < 0.001 versus Intact IVDs.

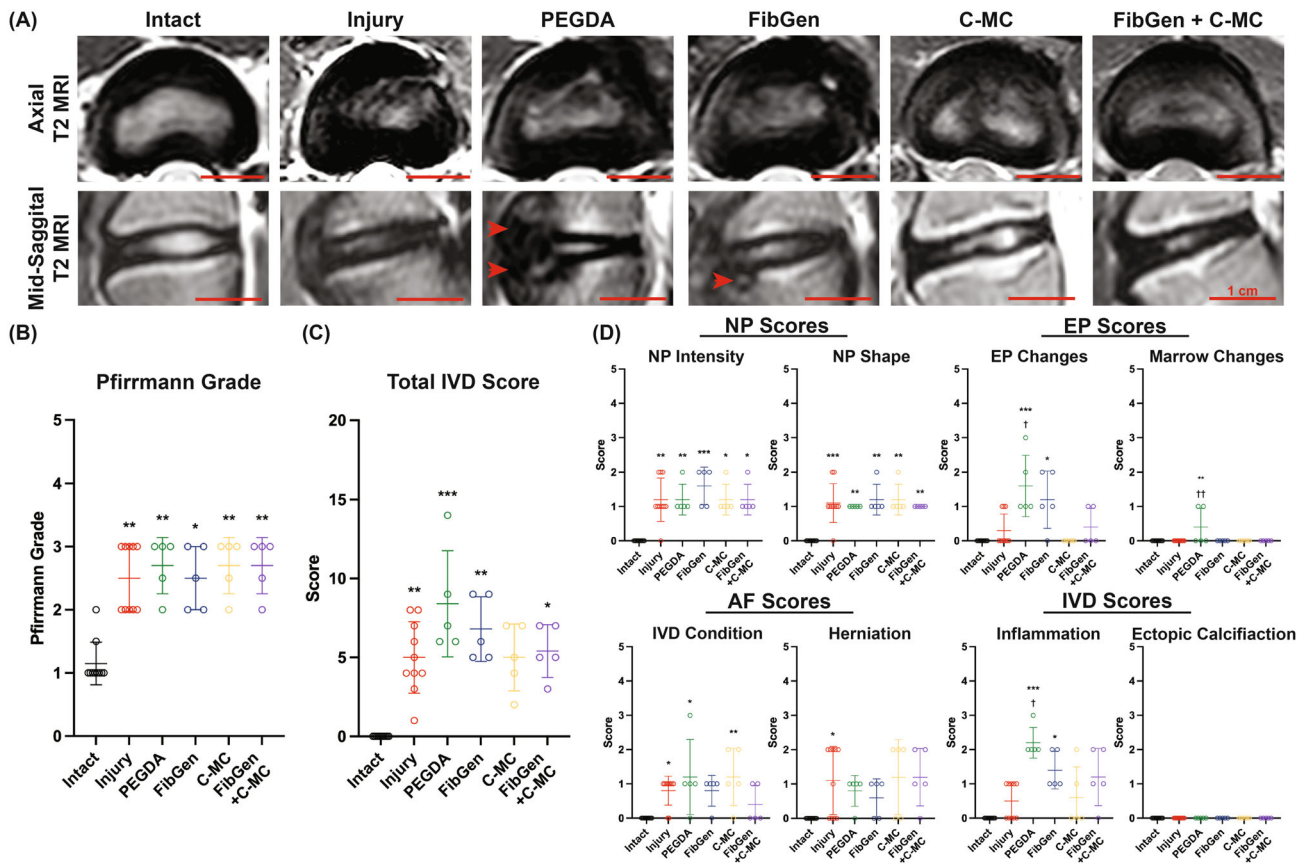


**FIGURE 3** Repaired and Injured IVDs are similar by Pfirrmann grade, but PEGDA and FibGen IVDs show increased local degeneration by detailed MR scoring. (A) Representative axial and mid-sagittal T2-weight magnetic resonance (MR) images. Red arrows indicate radiographic signs of endplate (EP) damage. Scale bar = 1 cm. (B) Pfirrmann grading. (C) Total IVD score using criteria from Table 1. (D) Individual IVD region scores using criteria from Table 1. Individual scores were summed together for the Total IVD Score in (C). \**p* < 0.05, \*\**p* < 0.01, and \*\*\**p* < 0.001 versus Intact IVDs. †*p* < 0.05; ††*p* < 0.01 versus Injury IVDs.

Comprehensive MR images used a scoring system that quantified changes in NP, AF, IVD, herniation, EP, marrow, and inflammation (Table 1). Compared to Intact IVDs, Injury IVDs had a significantly greater Total IVD Score, which was the summation of all individual

categories, demonstrating that the partial discectomy injury induced degenerative changes detectable by MR imaging (Figure 3C). PEGDA, FibGen, and FibGen + C-MC IVDs had significantly increased Total IVD scores compared to Intact IVDs, indicating that these repair



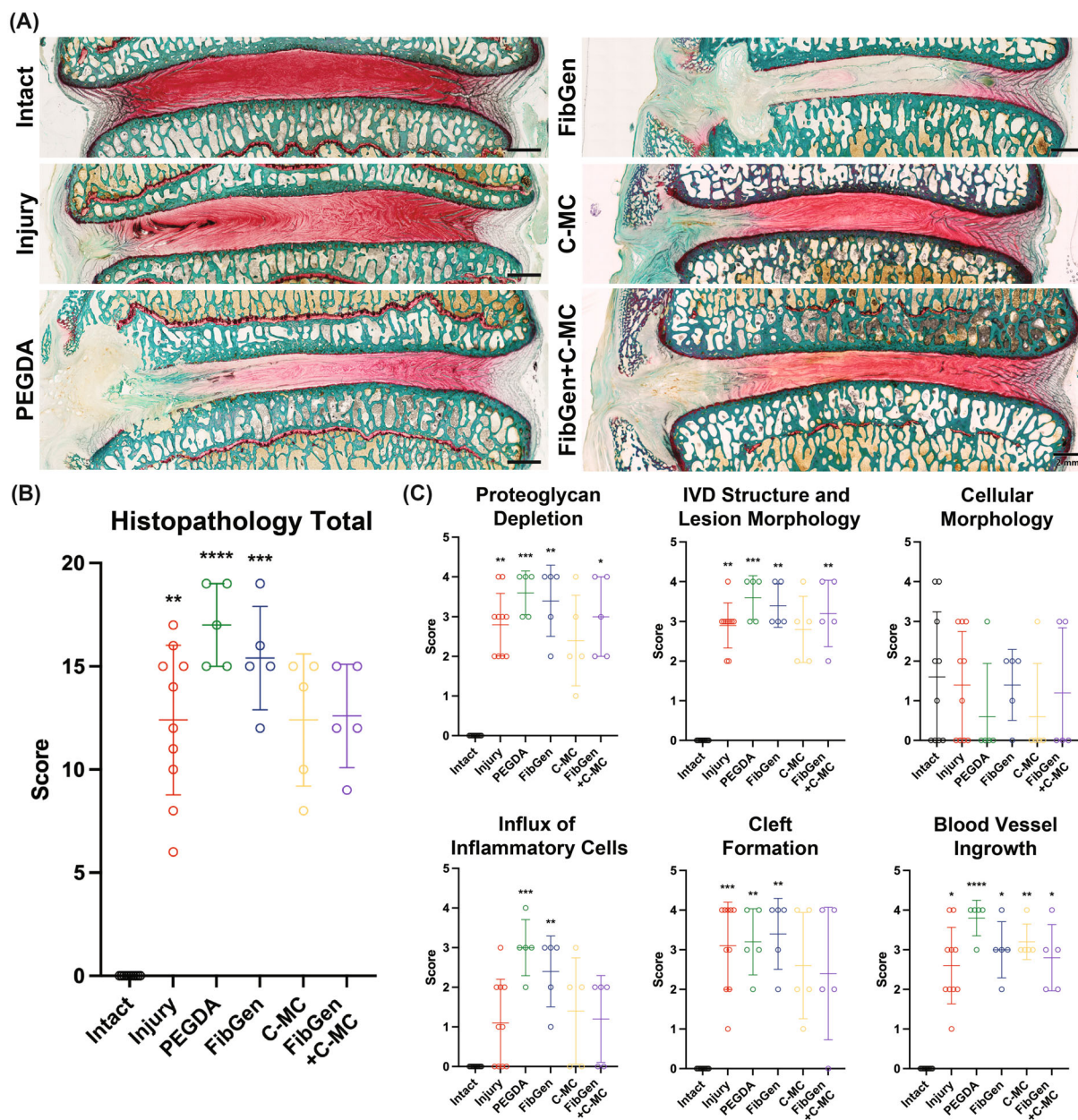


**FIGURE 4** C-MC and FibGen + C-MC IVDs show the least histopathological signs of degeneration. (A) Representative Safranin-O/Fast Green staining at W12 in the dorsal plane (nondecalfied, resin-embedded; left is ventrolateral and bottom is caudal). AF lamellae are highly aligned in Intact IVDs, compared to Injury, PEGDA, FibGen, C-MC, and FibGen + C-MC IVDs. Scale bar = 2 mm. (B) Semiquantitative analysis of Total Histopathological Score using Shu scoring system. (C) Semiquantitative analysis of individual categories for histopathological findings using the Shu scoring system. \* $p < 0.05$ , \*\* $p < 0.01$ , \*\*\* $p < 0.001$ , and \*\*\*\* $p < 0.0001$  versus Intact IVDs.

biomaterials could not prevent or reverse degenerative changes caused by partial discectomy injury. C-MC hydrogels were the only repair biomaterial that did not cause a significant increase in Total IVD score; however, this group did show a trending increase in Total IVD score ( $0.10 < p < 0.05$ ).

PEGDA and FibGen IVDs, the adhesive AF repair hydrogels in our study, caused degenerative IVD changes that were not found in Injury IVDs (Figure 3D). These degenerative changes were most prevalent for PEGDA IVDs. PEGDA IVDs had significantly greater scores than Injury IVDs for EP Changes, Marrow Changes, and Inflammation.

FibGen did not have significantly greater scores than Injury IVDs for any category; however, FibGen did cause significant EP Changes and Inflammation, compared to Intact IVDs. Since the PEGDA and FibGen formulations used in this study have unique chemical and mechanical properties, the presence of similar IVD degeneration in both groups was likely caused by their adhesive properties. Specifically, we hypothesize that direct contact of these adhesive hydrogels with the EP was responsible for causing accelerated IVD degeneration because these signs of degeneration were not present in IVDs that had nonadhesive C-MC injected into the central NP, in direct contact with the

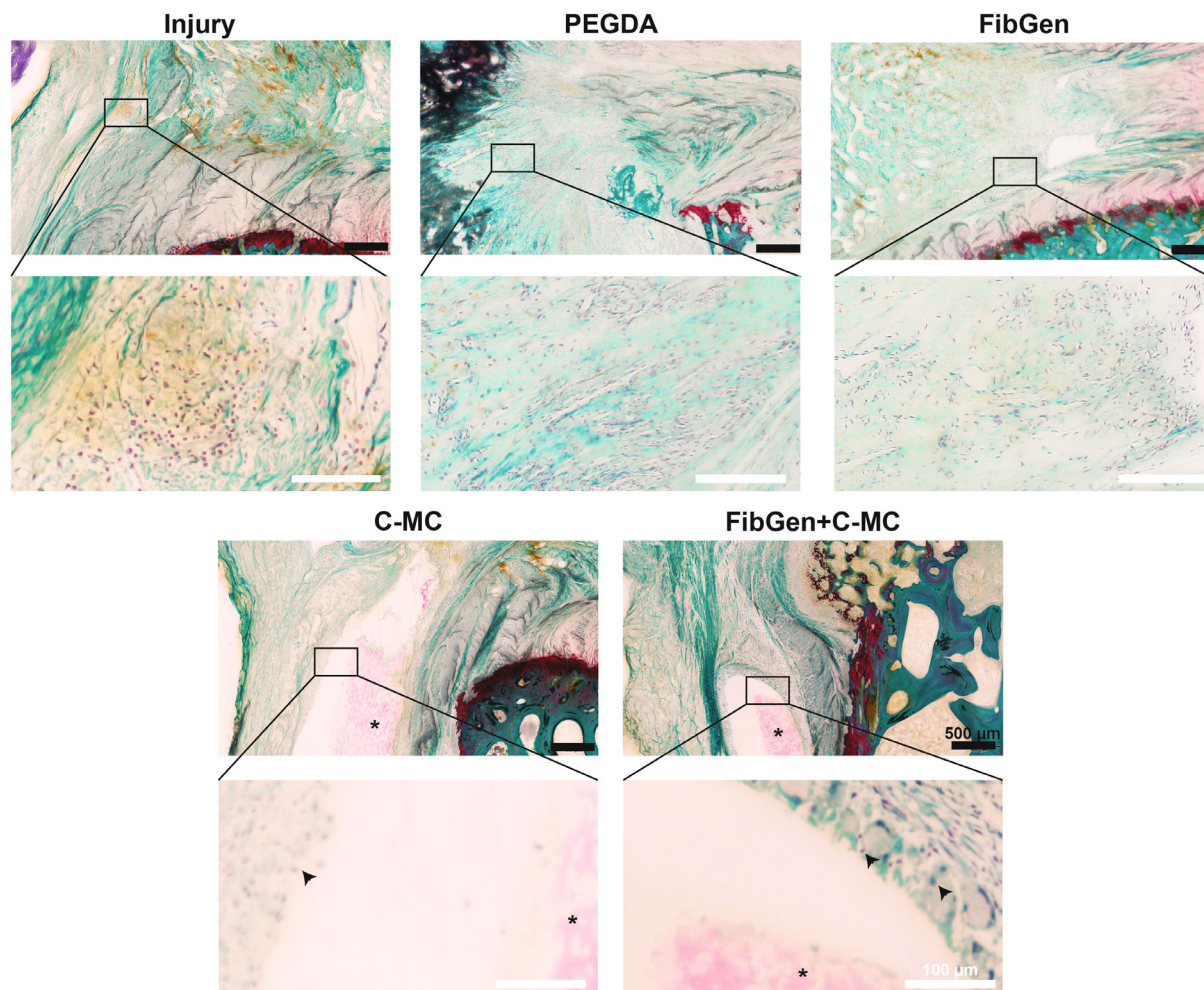


**FIGURE 5** Histopathological evaluation showed predominantly lymphocytic inflammation in PEGDA and FibGen IVDs, compared to histiocytic inflammation in C-MC and FibGen + C-MC IVDs. Representative inflammatory cell influx observed during histopathological staining at W12. Injury, PEGDA, and FibGen, IVDs showed lymphocytic cells, with round nuclei, aggregated to small follicles near blood vessels. C-MC and FibGen + C-MC IVDs showed histiocytic cells, with irregular shapes and peripherally located nuclei. Histiocytic cells (arrowhead) were aggregated around or near the foreign C-MC material (asterisk), which formed fluid-filled cysts. Representative images are shown at lower magnification (top, scale bar = 500  $\mu$ m) with a section (rectangle) shown at higher magnification (bottom, scale bar = 100  $\mu$ m).

EP (i.e., C-MC and FibGen + C-MC IVDs). These results suggest that combining a nonadhesive NP replacement biomaterial (i.e., C-MC) with an adhesive AF sealant (i.e., FibGen) could reduce the risk of degeneration.

### 3.4 | PEGDA and FibGen IVDs have greatest degeneration but lowest herniation risk

Partial discectomy resulted in Injury IVDs having significantly greater Total Histopathological Score than Intact IVDs (Figure 4B). The structural signs of degeneration for Injury IVDs included distortions of the AF lamellar structure, AF cleft formation, depletion of NP proteoglycan content, morphological changes to the EP, and vertebral bodies, and blood vessel ingrowth (Figure 4A). PEGDA, FibGen, C-MC, and FibGen + C-MC shared similar signs of structural degeneration with

Injury IVDs, but the incidences and severities of these features varied. As a result, the Total IVD Score for PEGDA and FibGen IVDs was significantly greater than Intact IVDs (Figure 4B). Based on individual subcategories that made up the Total Histopathology Score, these differences were driven mainly by more significant changes in the influx of inflammatory cells and cleft formation (Figure 4C). For these subcategories, PEGDA and FibGen IVDs had significantly greater scores than Intact IVDs, while there were no significant differences between Intact, C-MC, and FibGen + C-MC IVDs. Given these results, further analyses were focused on characterizing the inflammation and vertebral changes.

The influx of inflammatory cells was a consistent finding among Injury and repaired IVDs; however, the type of inflammatory cells and inflammation severity varied by condition. Injury, PEGDA, and FibGen IVDs all primarily experienced lymphocytic inflammation (Figure 5), yet PEGDA and FibGen IVDs mostly experienced a greater incidence



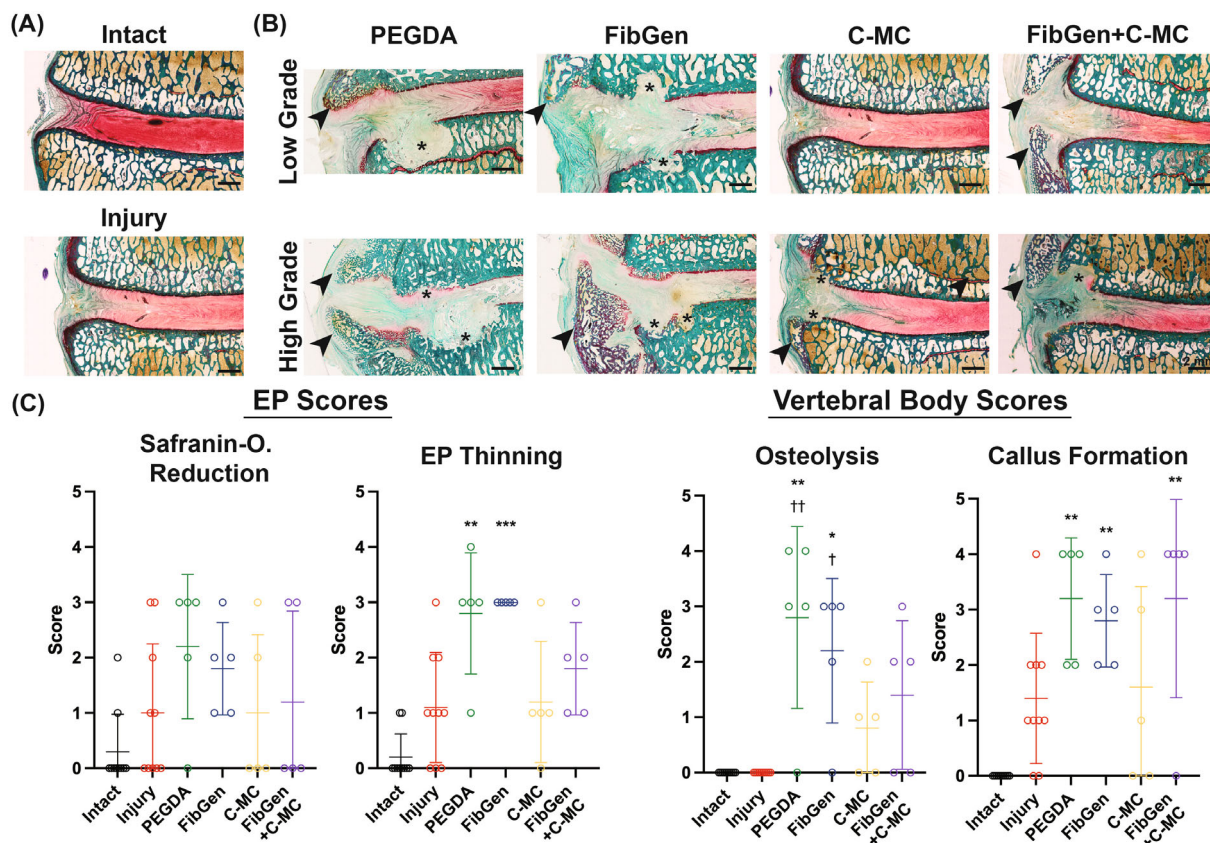


**FIGURE 6** Histopathological evaluation of EP and vertebral body showed greater damage in PEGDA and FibGen IVDs compared to C-MC and FibGen + C-MC IVDs. (A) Representative Safranin-O/Fast Green images of Intact and Injury IVDs at W12, which had no osteolysis. (B) Representative Safranin-O/Fast Green images of PEGDA, FibGen, C-MC, and FibGen + C-MC IVDs at W12 with varying severity of osteolysis. For each repair, top row images are the lowest grade and bottom row images are the highest grade observed in each group. All images were captured in the dorsal plane (non-decalcified, resin-embedded; left is ventrolateral and bottom is caudal). Scale bar = 2 mm. Asterisks mark left-sided destruction of the trabecular bone tissue and arrowheads mark focal formations in the vertebral bone. (C) Semiquantitative analysis of EP and vertebral bone parameters. \* $p < 0.05$ , \*\* $p < 0.01$ , \*\*\* $p < 0.001$ , and \*\*\*\* $p < 0.0001$  versus Intact IVDs. † $p < 0.05$  and †† $p < 0.01$  versus Injury IVDs.

of moderate, large, and extensive influx of inflammatory cells (100%,  $n = 5/5$  IVDs for PEGDA; 80%,  $n = 4/5$  IVDs for FibGen) compared to Injury IVDs (40%,  $n = 4/10$  IVDs for Injury). C-MC and FibGen + C-MC IVDs experienced histiocytic inflammation of monocyte and macrophage cells (Figure 5). Histiocytic cells were often found near cystic structures enclosing a foreign material located near or entirely outside the AF, which stained red. Since these cystic structures were only found in the C-MC and FibGen + C-MC IVDs, they were interpreted as remnants of dislocated or herniated C-MC material. The incidence of moderate and large influx of inflammatory cells was lower in C-MC and FibGen + C-MC IVDs (60%,  $n = 3/5$  IVDs for C-MC; 60%,  $n = 3/5$  IVDs for FibGen + C-MC), and not significantly different than Intact or Injury IVDs.

Vertebral bone changes were observed in all repaired IVDs, but not Injury IVDs, suggesting that the IVD repair biomaterials caused varying degrees of vertebral bone damage (Figure 6A,B). When present, vertebral osteolysis resulted in the formation of ovoid areas filled with soft tissue. This soft tissue was fibrous, contained high amounts of blood vessels, and had few inflammatory cells. PEGDA

and FibGen IVDs experienced the highest incidence (80%,  $n = 4/5$  for PEGDA IVDs; 80%,  $n = 4/5$  IVDs for FibGen) and severity of vertebral body osteolysis, which was significantly greater than Intact and Injury IVDs (Figure 6C). Vertebral body osteolysis in these conditions was characterized by focal discontinuation of the EPs and destruction of the underlying vertebral bone tissue. C-MC and FibGen + C-MC IVDs experienced lower severity vertebral osteolysis at lower incidences (60%,  $n = 3/5$  IVDs for C-MC; 60%,  $n = 3/5$  IVDs for FibGen + C-MC), and these were not statistically different than Intact IVDs. In addition, vertebral callus formation and periosteal reaction, characterized by periosteal proliferation of trabecular bone, were recorded in minimal to moderate severity in all treated IVDs.

Although PEGDA and FibGen IVDs had the most severe EP damage and inflammation, these IVDs also best-prevented reherniation in our partial discectomy model. Injury IVDs showed NP tissue herniation at the AF defect site in half of the samples (50%,  $n = 5/10$  IVDs) created during the partial discectomy injury (Figures 3 and 7). This NP tissue herniation was not observed in C-MC IVDs; however, expulsion of the C-MC biomaterial from the IVD space was observed (40%,

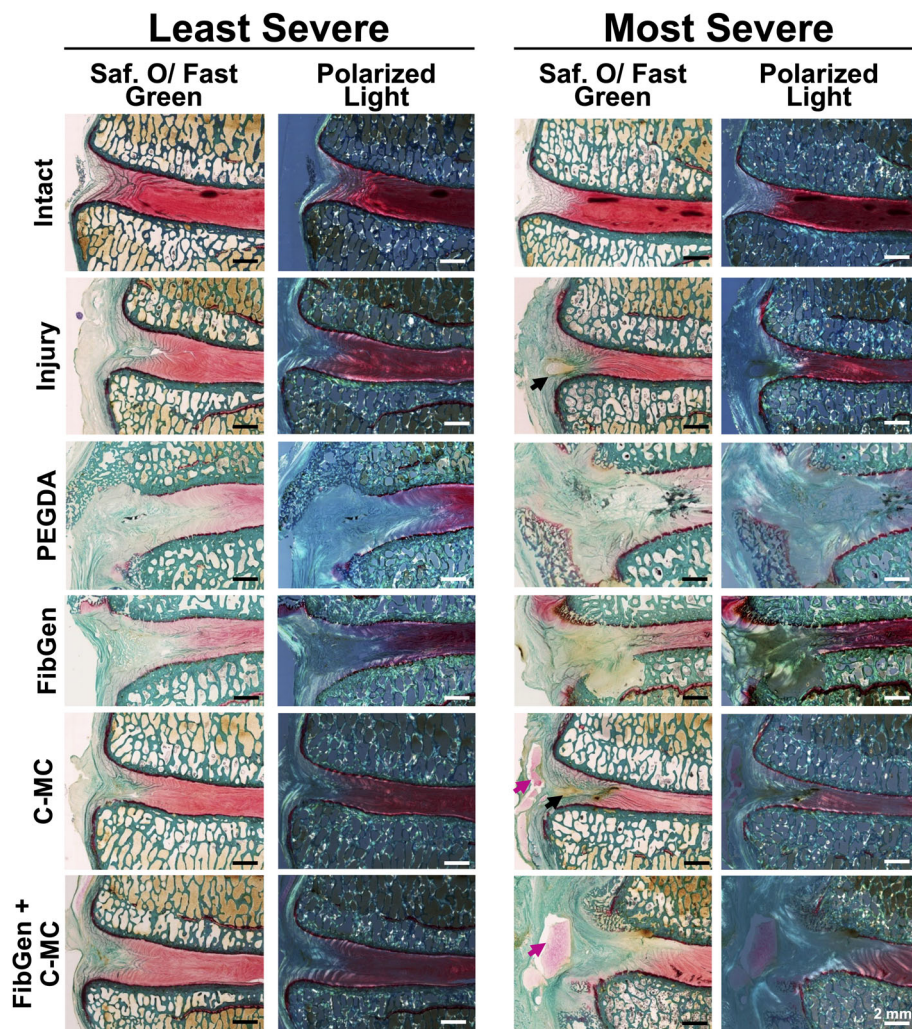


**FIGURE 7** PEGDA and FibGen AF sealants prevent NP herniation and did not experience biomaterial expulsion. Representative Safranin-O/Fast Green and polarized light images of Intact, Injury, PEGDA, FibGen, C-MC, and FibGen + C-MC IVDs at W12 with varying severity of NP herniation or biomaterial expulsion. For each repair, left column images are the least severely herniated and right column images are the most severely herniated IVDs observed in each group. All images were captured in the dorsal plane (non-decalcified, resin-embedded; left is ventrolateral and bottom is caudal). Black arrows indicate herniated NP material and pink arrows indicate C-MC expulsion. Scale bar = 2 mm.

$n = 2/5$  IVDs). Repair with adhesive AF sealants (i.e., PEGDA and FibGen) showed no histopathological signs of NP herniation or biomaterial herniation, which indicates that these biomaterials served their function of sealing AF defects and preventing reherniation. Although FibGen could prevent NP herniation, the AF sealant could not completely prevent herniation of C-MC in all cases because there were some incidences of C-MC biomaterial expulsion in FibGen + C-MC IVDs. Overall, results demonstrate that PEGDA and FibGen are effective AF sealants that can prevent reherniation of NP tissue. Histopathology results were complementary to herniation results by MR imaging (Figure 3D), although histopathology results were considered more definitive since the high water content from inflammation was not fully discernable from biomaterial expulsion with clinical MR imaging.

#### 4 | DISCUSSION

This study evaluated whether four treatments, using three injectable biomaterials, in an *in vivo* ovine discectomy model were capable of slowing IVD degeneration and resisting herniation. Skeletally mature

sheep experienced partial discectomy injury, which created a large, critically sized AF defect. This injury was then repaired using PEGDA, FibGen, C-MC, and FibGen + C-MC hydrogels. These non-bioactive biomaterials were chosen because they are tunable, cyto-compatible, and showed promising results in *ex vivo* models. We hypothesized that repair with these experimental biomaterials would prevent disc height loss and prevent IVD degeneration. Results showed that none of the tested IVD repair hydrogels could prevent injury-induced disc height loss or increases in Pfirrmann grade, and repaired IVDs were noninferior to Injury IVDs. This is an important benchmark since our Injury IVDs mimic partial discectomy, which is the current standard of care for symptomatic IVD herniation. PEGDA and FibGen, the adhesive hydrogel formulations in this study, had little risk of herniation or biomaterial expulsion; however, they caused EP changes and additional inflammation, which were not found in Injury IVDs. C-MC and FibGen + C-MC IVDs showed few EP changes on MR imaging and histopathology, showing that this EP damage may be mitigated by placing a nonadhesive hydrogel in contact with the EP. However, C-MC displayed some risk of biomaterial expulsion since it is a nonadhesive NP repair biomaterial. Overall, our data shows that C-MC and FibGen + C-MC



hydrogels continue to show promise for repairing injured IVDs, and that bioactive formulations could enhance their regenerative potential.

There were no clinically meaningful differences in IVD height loss between Injury IVDs and all repaired IVDs. Disc height is very sensitive to IVD damage and degeneration, and disc height loss is correlated with pain and disability<sup>6</sup>; thus, successful IVD repair biomaterials should aim to restore injury-induced disc height loss.<sup>52</sup> None of the repaired IVDs experienced injury-induced disc height loss immediately postoperatively at W0 and all IVDs experienced a slight increase in disc height. IVD swelling, disruption of the surrounding soft tissue, and effects from the anesthesia likely caused the disc height increases. By W4, all repaired IVDs experienced disc height loss. C-MC IVDs consistently had significantly lower disc height than Intact IVDs, which was expected since C-MC is a nonadhesive hydrogel.<sup>32</sup> C-MC biomaterial expulsion was also observable by histopathological analysis. PEGDA, FibGen, and FibGen + C-MC IVDs also experienced significant disc height loss compared to Intact IVDs; however, this was not consistent at all time points. For example, disc height for FibGen + C-MC IVDs was not significantly different than Intact IVDs at W4. Though not statistically significant, these differences always had trending significance ( $0.10 < p < 0.05$ ), and there were no biologically meaningful differences between groups. Of note, all repair IVDs maintained 90%–95% of their original disc height, indicating that the injury did not result in severe degeneration for any groups.

Histopathological and MRI degeneration grades were similar for Injury and all IVD repair biomaterials, suggesting these nonbioactive biomaterial formulations are not capable of slowing progressive IVD degeneration following injury. Augmentation with cells or bioactive components would be required for additional repair. Exogenous cells are considered beneficial because they can promote extracellular matrix synthesis, secrete paracrine signals that stimulate endogenous IVD cell anabolism, and release immunomodulatory signals to combat inflammation.<sup>53–55</sup> Injectable biomaterials can be modified for delivering cells to the IVD, and hydrogel formulations have the potential to simultaneously promote biomechanical and biological repair.<sup>53</sup> Several clinical trials have demonstrated that cell therapy using injectable hydrogel vehicles is safe and feasible for targeting the NP,<sup>55–57</sup> and it is expected that more clinical trials will arise. C-MC and FibGen + C-MC were most similar to Injury IVDs, with very little EP damage. Therefore, these hydrogels show most promise for continuing development to add bioactivity. There was some risk of biomaterial expulsion for C-MC even when combined with an AF sealant in the FibGen + C-MC group; therefore, further optimizations in biomaterial design and injection methods would be required. FibGen and C-MC have undergone extensive *in vitro* and *ex vivo* testing to demonstrate their feasibility as cell delivery biomaterials.<sup>30,31,45,46,58–63</sup> Future studies will be required for all tested biomaterials to assess whether delivering cells or mesenchymal stem cell-derived exosomes *in vivo* can better slow degeneration and promote IVD repair.

Adhesive hydrogels (i.e., PEGDA and FibGen) had no observable NP herniation or biomaterial expulsion, yet they caused EP damage, marrow changes, and inflammation compared to Injury IVDs. This

represents a novel finding that IVD repair with adhesive hydrogels can cause damage to the EP and vertebral bone. One hypothesis to explain this phenomenon is that *in situ* curing of PEGDA and FibGen induced aberrant stresses at the EP, such as tension and shear, since crosslinking during gelation can induce hydrogel network shrinkage due to molecular packing.<sup>64–66</sup> The effects of these mechanical stresses may be exacerbated under repetitive loading, contributing to the observed EP and vertebral tissue damage with inflammation. While the EP is known to be highly sensitive to aberrant loading conditions, dental resins, which are highly adhesive materials and also subject to repetitive long-term loading, are also associated with tooth fracture *in vivo*.<sup>67–69</sup> Therefore, the literature suggests that bone may be susceptible to adhesive biomaterials under repetitive loading conditions *in vivo*, and the EP damage, inflammation, and osteolysis in this study may have mechanical origins. Nevertheless, we highlight that Pfirrmann's grading was similar for Injury and all repaired IVDs, indicating that the observed EP defects and osteolysis were localized and did not result in a clinically meaningful degeneration. Long duration studies and additional time points will be required to determine whether these EP defects and inflammatory responses in PEGDA and FibGen IVDs will resolve or predispose to progressive degeneration over time.

Research and development of injectable adhesives for AF sealing is a promising strategy for minimizing the risk of herniation after discectomy. In a recent study, researchers repaired an ovine model of discectomy with an adhesive photocrosslinked collagen hydrogel, a nonadhesive hyaluronic acid NP replacement hydrogel, or a combination of both.<sup>44</sup> Interestingly, this study reported no significant changes in the EP or vertebral bodies for their collagen-only group, despite similarities in the placement of this hydrogel and our PEGDA and FibGen hydrogels. However, it is important to note that differences in hydrogel mechanical compliance under dynamic loading, endogenous cell infiltration, tissue remodeling, and inflammatory responses may also impact these outcomes. Despite the local EP defects and osteolysis observed when using PEGDA and FibGen, without C-MC combination, the adhesives demonstrated efficacy in preventing NP herniation and withstanding biomaterial expulsion. This underscores the potential of these hydrogels to enhance IVD procedure outcomes, given the biomaterial design and injection methods are optimized to reduce vertebral damage.

Although this study helped advance a novel strategy for treating discectomy, it was not without limitations. First, histopathologic grading was conducted using ranked integers, as is common practice for large animal IVD studies.<sup>50,70</sup> However, more complex statistical methods (e.g. principal component analysis) could be useful in determining which grading categories were most important. Second, we could not fully discern why different biomaterials resulted in different types of inflammation. The reduced influx of inflammatory cells in response to C-MC containing implants compared to PEGDA and FibGen alone may be due to the reported anti-fouling properties of MC, which has been shown to limit plasmatic protein adsorption and subsequent adhesion by tissue and bacterial cells.<sup>71</sup> It is possible that the anti-fouling nature of MC may mitigate leukocyte adhesion and the associated foreign body reaction to the C-MC hydrogels. Still,



more long-term evaluation will be required to ascertain whether there is complete resolution of the histiocytic inflammatory response to the various biomaterials. Lastly, while our study was sufficiently powered to detect large differences between groups, we would have required a larger sample size to determine more modest differences. This is a common issue with costly large animal studies.

Large animal studies are ethically and economically costly; therefore, we evaluated biomaterials that had undergone extensive *in vitro*, *ex vivo*, and small animal testing. Interestingly, detrimental mechanical effects were not captured in our previous *ex vivo* studies with FibGen (with testing up to 96 000 cycles for 1 week).<sup>40,58</sup> We therefore highlight the need for large animal *in vivo* testing for advanced validation studies, since even the most rigorous organ culture studies do not fully simulate the immune system or repetitive loading environment *in vivo*. This large animal model, and most large animal studies, was designed for validation studies and not intended to establish deeper mechanistic comparisons across groups. We believe that since EP damage was observed from two highly distinct adhesive formulations, and that damage was mostly mitigated by our FibGen + C-MC composite repair, the EP damage was caused by aberrant stresses on the EP from adhesive forces. Nevertheless, it is possible that there are distinct mechanisms of EP damage and osteolysis occurring in these biomaterial strategies. In this study, Injury IVDs received a partial discectomy injury with NP removal to simulate the clinical standard of care for symptomatic IVD herniation. We expect that an AF defect without NP removal would have resulted in more severe herniations for Injury IVDs.

## 5 | CONCLUSION

This study tested whether three experimental, injectable IVD repair biomaterials (i.e., PEGDA, FibGen, and C-MC) could slow IVD degeneration in a clinically relevant ovine discectomy model. No biomaterial strategy could prevent discectomy-associated disc height loss at W12; however, all repaired IVDs retained upwards of 90% of their preoperative disc height. Pfirrmann grading was also similar for Injury and all repaired IVDs. These results indicate that our repair biomaterials were not inferior to the clinical standard of care for symptomatic IVD herniation and that using these materials for delivery of bioactive factors would be a useful next step to enhance IVD healing. We identified a novel finding that IVDs repaired with only adhesive AF repair biomaterials (i.e., PEGDA and FibGen) had severe localized EP changes and inflammation, which were observable by MR and histopathological analyses. Importantly, these adhesive AF sealants did not exhibit NP herniation or biomaterial expulsion. These degenerative changes were less severe or not present in C-MC and FibGen + C-MC IVDs, suggesting that combining nonadhesive NP repair biomaterials (i.e., C-MC) with AF sealants show most promise for discectomy repair. We also highlight that a large animal *in vivo* test was necessary to identify such damage, which was not present in prior biomaterial testing since small animals and organ cultures are unlikely to have sufficient inflammatory and repetitive loading environments to induce this localized

EP damage. Future studies can therefore focus on exploring the mechanisms by which adhesive hydrogels cause damage to the EP and vertebral bodies, and on augmenting biomaterial strategies with cells or other bioactive factors to attenuate inflammation and better promote repair.

## ACKNOWLEDGMENTS

This work was supported by the National Institutes of Health (NIH) National Institute of Arthritis and Musculoskeletal and Skin Diseases (NIAMS) grants R01 AR057397 [JCI], R01 AR080096 [JCI], and F31 AR077385 [CJP], the AO Foundation, and AO Spine. Authors would like to thank Nora Goudsouzian (AO Research Institute Davos) and Damien Laudier (Icahn School of Medicine at Mount Sinai) for their assistance with histopathology. Authors would also like to acknowledge Dr. Jashvant Poeran for statistical consultations and Jill Gregory for medical illustrations.

## ORCID

Christopher J. Panebianco  <https://orcid.org/0000-0001-8683-5743>

Caroline Constant  <https://orcid.org/0000-0002-7846-5612>

Andrea J. Vernengo  <https://orcid.org/0000-0002-5143-7435>

Dirk Nehrbass  <https://orcid.org/0000-0002-4871-5473>

Dominic Gehweiler  <https://orcid.org/0000-0001-7148-9569>

Tyler J. DiStefano  <https://orcid.org/0000-0001-9406-3085>

David J. Alpert  <https://orcid.org/0000-0002-7124-5457>

Saad B. Chaudhary  <https://orcid.org/0000-0002-5305-3785>

Andrew C. Hecht  <https://orcid.org/0000-0001-5228-4568>

Alan C. Seifert  <https://orcid.org/0000-0001-7877-4813>

Steven B. Nicoll  <https://orcid.org/0000-0001-9832-9151>

Sibylle Grad  <https://orcid.org/0000-0001-9552-3653>

Stephan Zeiter  <https://orcid.org/0000-0002-8155-4202>

James C. Iatridis  <https://orcid.org/0000-0002-2186-0590>

## REFERENCES

- Lo J, Chan L, Flynn S. A systematic review of the incidence, prevalence, costs, and activity and work limitations of amputation, osteoarthritis, rheumatoid arthritis, back pain, multiple sclerosis, spinal cord injury, stroke, and traumatic brain injury in the United States: a 2019 update. *Arch Phys Med Rehabil.* 2021;102:115-131.
- Ravindra VM, Senglaub SS, Rattani A, et al. Degenerative lumbar spine disease: estimating global incidence and worldwide volume. *Global Spine J.* 2018;8:784-794.
- Vlaeyen JWS, Maher CG, Wiech K, et al. Low back pain. *Nat Rev Dis Primers.* 2018;4:52.
- Ito K, Creemers L. Mechanisms of intervertebral disk degeneration/injury and pain: a review. *Global Spine J.* 2013;3:145-152.
- Yang H, Haldeman S. Behavior-related factors associated with low Back pain in the US adult population. *Spine.* 2018;43:28-34.
- Hartvigsen J, Hancock MJ, Kongsted A, et al. What low back pain is and why we need to pay attention. *Lancet.* 2018;391:2356-2367.
- Anema JR, Schellart AJM, Cassidy JD, Loisel P, Veerman TJ, van der Beek AJ. Can cross country differences in return-to-work after chronic occupational back pain be explained? An exploratory analysis on disability policies in a six country cohort study. *J Occup Rehabil.* 2009;19:419-426.
- Ma VY, Chan L, Carruthers KJ. Incidence, prevalence, costs, and impact on disability of common conditions requiring rehabilitation in

- the United States: stroke, spinal cord injury, traumatic brain injury, multiple sclerosis, osteoarthritis, rheumatoid arthritis, limb loss, and back pain. *Arch Phys Med Rehabil*. 2014;95:986-995.e1.
9. Dieleman JL, Cao J, Chapin A, et al. US Health Care spending by payer and health condition, 1996-2016. *JAMA*. 2020;323:863-884.
  10. Weinstein JN, Lurie JD, Tosteson TD, et al. Surgical versus nonoperative treatment for lumbar disc herniation: four-year results for the Spine Patient Outcomes Research Trial (SPORT). *Spine*. 2008;33:2789-2800.
  11. Lurie JD, Tosteson TD, Tosteson ANA, et al. Surgical versus nonoperative treatment for lumbar disc herniation: eight-year results for the spine patient outcomes research trial. *Spine*. 2014;39:3-16.
  12. Tosteson ANA, Tosteson TD, Lurie JD, et al. Comparative effectiveness evidence from the spine patient outcomes research trial: surgical versus nonoperative care for spinal stenosis, degenerative spondylolisthesis, and intervertebral disc herniation. *Spine*. 2011;36:2061-2068.
  13. Carragee EJ, Han MY, Suen PW, Kim D. Clinical outcomes after lumbar discectomy for sciatica: the effects of fragment type and annular competence. *J Bone Joint Surg Am*. 2003;85:102-108.
  14. McGirt MJ, Eustacchio S, Varga P, et al. A prospective cohort study of close interval computed tomography and magnetic resonance imaging after primary lumbar discectomy: factors associated with recurrent disc herniation and disc height loss. *Spine*. 2009;34:2044-2051.
  15. Ahn Y, Lee S-H, Lee JH, Kim JU, Liu WC. Transforaminal percutaneous endoscopic lumbar discectomy for upper lumbar disc herniation: clinical outcome, prognostic factors, and technical consideration. *Acta Neurochir*. 2009;151:199-206.
  16. Parker SL, Grahovac G, Vukas D, et al. Effect of an annular closure device (Barricaid) on same-level recurrent disk herniation and disk height loss after primary lumbar discectomy: two-year results of a multicenter prospective cohort study. *Clin Spine Surg*. 2016;29:454-460.
  17. Nanda D, Arts MP, Miller LE, et al. Annular closure device lowers reoperation risk 4 years after lumbar discectomy. *Med Devices*. 2019;12:327-335.
  18. Kienzler JC, Fandino J, van de Kelft E, Eustacchio S, Bouma GJ, The Barricaid® Annular Closure RCT Study Group. Risk factors for early reherniation after lumbar discectomy with or without annular closure: results of a multicenter randomized controlled study. *Acta Neurochir*. 2021;163:259-268.
  19. Bowles RD, Setton LA. Biomaterials for intervertebral disc regeneration and repair. *Biomaterials*. 2017;129:54-67.
  20. Long RG, Torre OM, Hom WW, Assael DJ, Iatridis JC. Design requirements for annulus fibrosus repair: review of forces, displacements, and material properties of the intervertebral disk and a summary of candidate hydrogels for repair. *J Biomech Eng*. 2016;138:021007.
  21. Iatridis JC, Nicoll SB, Michalek AJ, Walter BA, Gupta MS. Role of biomechanics in intervertebral disc degeneration and regenerative therapies: what needs repairing in the disc and what are promising biomaterials for its repair? *Spine J*. 2013;13:243-262.
  22. Allen MJ, Schoonmaker JE, Bauer TW, Williams PF, Higham PA, Yuan HA. Preclinical evaluation of a poly (vinyl alcohol) hydrogel implant as a replacement for the nucleus pulposus. *Spine*. 2004;29:515-523.
  23. Richardson SM, Curran JM, Chen R, et al. The differentiation of bone marrow mesenchymal stem cells into chondrocyte-like cells on poly-L-lactic acid (PLLA) scaffolds. *Biomaterials*. 2006;27:4069-4078.
  24. Christiani T, Mys K, Dyer K, Kadlowec J, Iftode C, Vernengo AJ. Using embedded alginate microparticles to tune the properties of in situ forming poly(N-isopropylacrylamide)-graft-chondroitin sulfate bioadhesive hydrogels for replacement and repair of the nucleus pulposus of the intervertebral disc. *JOR Spine*. 2021;4:e1161.
  25. Vernengo J, Fussell GW, Smith NG, Lowman AM. Evaluation of novel injectable hydrogels for nucleus pulposus replacement. *J Biomed Mater Res Part B Appl Biomater*. 2008;84:64-69.
  26. Thomas JD, Fussell G, Sarkar S, Lowman AM, Marcolongo M. Synthesis and recovery characteristics of branched and grafted PNIPAAm-PEG hydrogels for the development of an injectable load-bearing nucleus pulposus replacement. *Acta Biomater*. 2010;6:1319-1328.
  27. Chou AI, Nicoll SB. Characterization of photocrosslinked alginate hydrogels for nucleus pulposus cell encapsulation. *J Biomed Mater Res A*. 2009;91:187-194.
  28. Burdick JA, Chung C, Jia X, Randolph MA, Langer R. Controlled degradation and mechanical behavior of photopolymerized hyaluronic acid networks. *Biomacromolecules*. 2005;6:386-391.
  29. Baer AE, Wang JY, Kraus VB, Setton LA. Collagen gene expression and mechanical properties of intervertebral disc cell-alginate cultures. *J Orthop Res*. 2001;19:2-10.
  30. Reza AT, Nicoll SB. Serum-free, chemically defined medium with TGFβ-3 enhances functional properties of nucleus pulposus cell-laden carboxymethylcellulose hydrogel constructs. *Biotechnol Bioeng*. 2010;105:384-395.
  31. Reza AT, Nicoll SB. Characterization of novel photocrosslinked carboxymethylcellulose hydrogels for encapsulation of nucleus pulposus cells. *Acta Biomater*. 2010;6:179-186.
  32. Lin HA, Varma DM, Hom WW, et al. Injectable cellulose-based hydrogels as nucleus pulposus replacements: assessment of in vitro structural stability, ex vivo herniation risk, and in vivo biocompatibility. *J Mech Behav Biomed Mater*. 2019;96:204-213.
  33. Lewis G. Nucleus pulposus replacement and regeneration/repair technologies: present status and future prospects. *J Biomed Mater Res Part B Appl Biomater*. 2012;100:1702-1720.
  34. Di Martino A, Vaccaro AR, Lee JY, Denaro V, Lim MR. Nucleus pulposus replacement: basic science and indications for clinical use. *Spine*. 2005;30:S16-S22.
  35. Chik TK, Ma XY, Choy TH, et al. Photochemically crosslinked collagen annulus plug: a potential solution solving the leakage problem of cell-based therapies for disc degeneration. *Acta Biomater*. 2013;9:8128-8139.
  36. Borde B, Grunert P, Härtl R, Bonassar LJ. Injectable, high-density collagen gels for annulus fibrosus repair: an in vitro rat tail model. *J Biomed Mater Res A*. 2015;103:2571-2581.
  37. Scheibler A-G, Götschi T, Widmer J, et al. Feasibility of the annulus fibrosus repair with in situ gelating hydrogels—a biomechanical study. *PLoS One*. 2018;13:e0208460.
  38. Kang R, Li H, Lysdahl H, et al. Cyanoacrylate medical glue application in intervertebral disc annulus defect repair: mechanical and biocompatible evaluation. *J Biomed Mater Res Part B Appl Biomater*. 2017;105:14-20.
  39. DiStefano TJ, Shmukler JO, Danias G, et al. Development of a two-part biomaterial adhesive strategy for annulus fibrosus repair and ex vivo evaluation of implant herniation risk. *Biomaterials*. 2020;258:120309.
  40. Likhitpanichkul M, Dreischarf M, Illien-Junger S, et al. Fibrin-genipin adhesive hydrogel for annulus fibrosus repair: performance evaluation with large animal organ culture, in situ biomechanics, and in vivo degradation tests. *Eur Cell Mater*. 2014;28:25-37; discussion 37.
  41. Guterl CC, Torre OM, Purmessur D, et al. Characterization of mechanics and cytocompatibility of fibrin-genipin annulus fibrosus sealant with the addition of cell adhesion molecules. *Tissue Eng Part A*. 2014;20:2536-2545.
  42. Long RG, Ferguson SJ, Benneker LM, et al. Morphological and biomechanical effects of annulus fibrosus injury and repair in an ovine cervical model. *JOR Spine*. 2020;3:e1074.
  43. Hom WW, Tschopp M, Lin HA, et al. Composite biomaterial repair strategy to restore biomechanical function and reduce herniation risk in an ex vivo large animal model of intervertebral disc herniation with varying injury severity. *PLoS One*. 2019;14:e0217357.
  44. Sloan SR, Wipplinger C, Kirnaz S, et al. Combined nucleus pulposus augmentation and annulus fibrosus repair prevents acute intervertebral

- disc degeneration after discectomy. *Sci Transl Med.* 2020;12. <https://doi.org/10.1126/scitranslmed.aay2380>
45. Panebianco CJ, DiStefano TJ, Mui B, Hom WW, Iatridis JC. Crosslinker concentration controls TGF $\beta$ -3 release and annulus fibrosus cell apoptosis in genipin-crosslinked fibrin hydrogels. *Eur Cell Matter.* 2020;39:211-226.
  46. Cruz MA, Hom WW, DiStefano TJ, et al. Cell-seeded adhesive biomaterial for repair of annulus fibrosus defects in intervertebral discs. *Tissue Eng Part A.* 2018;24:187-198.
  47. Varma DM, DiNicolas MS, Nicoll SB. Injectable, redox-polymerized carboxymethylcellulose hydrogels promote nucleus pulposus-like extracellular matrix elaboration by human MSCs in a cell density-dependent manner. *J Biomater Appl.* 2018;33:576-589.
  48. Constant C, Hom WW, Nehrbass D, et al. Comparison and optimization of sheep in vivo intervertebral disc injury model. *JOR Spine.* 2022;5:e1198.
  49. Pfirrmann CW, Metzendorf A, Zanetti M, Hodler J, Boos N. Magnetic resonance classification of lumbar intervertebral disc degeneration. *Spine.* 2001;26:1873-1878.
  50. Shu CC, Smith MM, Smith SM, Dart AJ, Little CB, Melrose J. A histopathological scheme for the quantitative scoring of intervertebral disc degeneration and the therapeutic utility of adult mesenchymal stem cells for intervertebral disc regeneration. *Int J Mol Sci.* 2017;18:1049.
  51. Cohen J. A coefficient of agreement for nominal scales. *Educ Psychol Meas.* 1960;20:37-46.
  52. Michalek AJ, Iatridis JC. Height and torsional stiffness are most sensitive to annular injury in large animal intervertebral discs. *Spine J.* 2012;12:425-432.
  53. Panebianco CJ, Meyers JH, Gansau J, Hom WW, Iatridis JC. Balancing biological and biomechanical performance in intervertebral disc repair: a systematic review of injectable cell delivery biomaterials. *Eur Cell Matter.* 2020;40:239-258.
  54. Burdick JA, Mauck RL, Gerecht S. To serve and protect: hydrogels to improve stem cell-based therapies. *Cell Stem Cell.* 2016;18:13-15.
  55. Sakai D, Andersson GBJ. Stem cell therapy for intervertebral disc regeneration: obstacles and solutions. *Nat Rev Rheumatol.* 2015;11:243-256.
  56. Schol J, Sakai D. Cell therapy for intervertebral disc herniation and degenerative disc disease: clinical trials. *Int Orthop.* 2019;43:1011-1025.
  57. Benneker LM, Andersson G, Iatridis JC, et al. Cell therapy for intervertebral disc repair: advancing cell therapy from bench to clinics. *Eur Cell Mater.* 2014;27:5-11.
  58. Panebianco CJ, Rao S, Hom WW, et al. Genipin-crosslinked fibrin seeded with oxidized alginate microbeads as a novel composite biomaterial strategy for intervertebral disc cell therapy. *Biomaterials.* 2022;287:121641.
  59. Gupta MS, Nicoll SB. Duration of TGF- $\beta$ 3 exposure impacts the chondrogenic maturation of human MSCs in photocrosslinked carboxymethylcellulose hydrogels. *Ann Biomed Eng.* 2015;43:1145-1157.
  60. Lin HA, Gupta MS, Varma DM, Gilchrist ML, Nicoll SB. Lower crosslinking density enhances functional nucleus pulposus-like matrix elaboration by human mesenchymal stem cells in carboxymethylcellulose hydrogels. *J Biomed Mater Res A.* 2016;104:165-177.
  61. Gupta MS, Cooper ES, Nicoll SB. Transforming growth factor-beta 3 stimulates cartilage matrix elaboration by human marrow-derived stromal cells encapsulated in photocrosslinked carboxymethylcellulose hydrogels: potential for nucleus pulposus replacement. *Tissue Eng Part A.* 2011;17:2903-2910.
  62. Gupta MS, Nicoll SB. Functional nucleus pulposus-like matrix assembly by human mesenchymal stromal cells is directed by macromer concentration in photocrosslinked carboxymethylcellulose hydrogels. *Cell Tissue Res.* 2014;358:527-539.
  63. Chou AI, Akintoye SO, Nicoll SB. Photo-crosslinked alginate hydrogels support enhanced matrix accumulation by nucleus pulposus cells in vivo. *Osteoarthr Cartil.* 2009;17:1377-1384.
  64. Pérez LA, Hernández R, Alonso JM, Pérez-González R, Sáez-Martínez V. Granular disulfide-crosslinked hyaluronic hydrogels: a systematic study of reaction conditions on thiol substitution and injectability parameters. *Polymers.* 2023;15. <https://doi.org/10.3390/polym15040966>
  65. Zhao Z, Wang C, Yan H, Liu Y. Soft robotics programmed with double crosslinking DNA hydrogels. *Adv Funct Mater.* 2019;29:1905911.
  66. Labella R, Lambrechts P, Van Meerbeek B, Vanherle G. Polymerization shrinkage and elasticity of flowable composites and filled adhesives. *Dent Mater.* 1999;15:128-137.
  67. Schneider LFF, Cavalcante LM, Silikas N. Shrinkage stresses generated during resin-composite applications: a review. *J Dent Biomech.* 2010;2010:131630.
  68. Dauvillier BS, Aarnts MP, Feilzer AJ. Developments in shrinkage control of adhesive restoratives. *J Esthet Dent.* 2000;12:291-299.
  69. van Ende A, de Munck J, Mine A, Lambrechts P, van Meerbeek B. Does a low-shrinking composite induce less stress at the adhesive interface? *Dent Mater.* 2010;26:215-222.
  70. Lee NN, Salzer E, Bach FC, et al. A comprehensive tool box for large animal studies of intervertebral disc degeneration. *JOR Spine.* 2021;4:e1162.
  71. Mussard W, Kebir N, Kriegel I, Estève M, Semetey V. Facile and efficient control of bioadhesion on poly(dimethylsiloxane) by using a biomimetic approach. *Angew Chem Int Ed.* 2011;50:10871-10874.

## SUPPORTING INFORMATION

Additional supporting information can be found online in the Supporting Information section at the end of this article.

**How to cite this article:** Panebianco, C. J., Constant, C., Vernengo, A. J., Nehrbass, D., Gehweiler, D., DiStefano, T. J., Martin, J., Alpert, D. J., Chaudhary, S. B., Hecht, A. C., Seifert, A. C., Nicoll, S. B., Grad, S., Zeiter, S., & Iatridis, J. C. (2023). Combining adhesive and nonadhesive injectable hydrogels for intervertebral disc repair in an ovine discectomy model. *JOR Spine*, 6(4), e1293. <https://doi.org/10.1002/jsp2.1293>